# What about the Tailpiece?

JACQUES PIGNERET

74 Rue d'Amblainvilliers, Verrieres le Buisson 91370, France
jpigneret@free.fr

## Abstract

*Although there are studies on positioning the tailpiece or choosing different essence of wood, the tailpiece still conceals its added values in the violin setup. Is it a simple string holder? This article studies the impact of the tailpiece on the mechanical energy collected by the bridge of a viola. A rig, which simulates a viola without a body, provides the measurements for this article. This work uses fine measurements of string, bridge, and tailpiece motions, which represent a wide range of geometrical and physical parameters. This article discusses data collected from a monocord, a one-string viola with a tailpiece, and two-string violas in both symmetric and asymmetrical connections. These data reveal the varying resonances and the phase reversal mechanism, which cause amplitude and sound tone modulations in bridge motion. This bridge motion is the source of body vibration. This article also demonstrates that the physical parameters of the tailpiece, as well as the attachment cord, have little effect on the resonances present within the bridge compared with the length of the after-strings (ASs). Selective lengthening of these ASs, when connected to an asymmetric tailpiece, can increase the partials of played notes without a significant impact on mean available energy.*

## PURPOSE OF THIS WORK

This article delves again into the problem of attaching after-length strings to the body of a bowed instrument. All stringed instruments need a way to support the tension of strings without compromising their structural integrity or adversely affecting their sound. Other instruments, such as the guitar, harp, and piano, incorporate unique solutions to this problem. In the case of the violin family, however, the tail cord or tailpiece plays this role. Previous works have documented the contribution of the after-length string system by analyzing the after-length string, the size of the tailpiece, the shape and mass of the tailpiece, and the length of the attached cord [1–3]. These articles focused mainly on analysis of the mechanical behavior that was present within several resonance modes. These covered a spectrum from below the lowest note played and up to 1 kHz. Researchers obtained these measurements through tapping techniques. These resonances are useful during the tuning process of any stringed instrument.

This article focuses on the "output" of the vibrations of the bridge, which is to say the intensity of sound, the richness of sound, and the ease of playing the instrument. Different inputs, determined by the physical parameters of the after-string (AS) system, can positively or negatively affect these qualities. As the size and shape of a tailpiece can affect the length of each AS, the tailpiece affects multiple aspects of the instrument.

Although modern digital simulators can describe some elements of this behavior, they cannot precisely model the friction which occurs between the hairs and string. In addition, these simulations cannot account for variations in stiffness of strings at the bridge notch at pitch. Therefore, we have used an experimental approach with an emphasis on precise, reproducible measurements. For this reason, this article also discards body contribution to focus on the driving forces on the bridge. To achieve these goals, this work uses a rigid wood dead rig, which records the forces acting on the top of the bridge as shown in Fig. 1.

The rig models a viola-sized (41 cm) instrument. It has fixed angles, string length, and tension which model an instrument of that size, but allows full freedom to adjust the position, mass, and three-dimensional inertia of the tailpiece. In addition, the tailpiece can connect to a single vibrating string or two vibrating strings. The
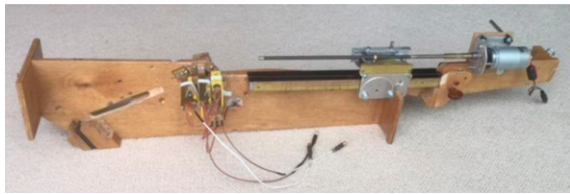
*Figure 1. Rigid wood-built rig.*

vibrating length is $L_{m0}$ = 375 mm, with a bridge to saddle distance of 200 mm.

This article uses data gathered from three rig configurations:

1. No tailpiece with a single string stretched from nut to saddle
2. Rigid tailpiece with variable tail cord types and lengths
3. Rigid tailpiece with two strings and variable after-lengths

Acronyms used in this article are listed in the Glossary.

## INSTRUMENTATION

The rig has a pseudo-bridge (BR), or string-holder, which replicates the bridge of a viola. Previous measurements of the static transverse stiffness ($K$) at the top bridges, taken across five violas, provide a range of $K$ = 20–30 N/mm. Testing violas with a dynanometer, operated by a calibrated spring, shows applied forces ($F$) in the range of 2–10 N on bridges. Using $dx$ under $dF$ derives a stiffness equation of $K = dF/dx$, measured in N/mm. These measurements correspond to violas with strings, a bridge alone with clamped feet, and the pseudo-bridge, as shown in Fig. 2.

The stiffness of the pseudo-bridge (holder) is adjusted by carving the rod, made from an epicea post. The mass, transverse resonance frequency, and Q are similar (~3 g, 1300 Hz, 22), as well as the admittance curve obtained by tapping techniques, to real bridges on viola. Forces on the holder have been recorded by a homemade quartz force sensor, horizontally, when in blocked mode (horizontal quartz force sensor [HFS]). Transverse displacements have been measured by homemade laser position sensors (LPS) (Fig. 3).

The added mass of the tiny tube modifies string vibrations, as do the wolf-eliminators placed on the ASs. In the latter case, the mass of the tube is much higher than that of the string. In our experiment, the tiny tube is a local perturbation, as would be an imperfect string. To evaluate this perturbation, we performed an experiment to determine the variations. We use a monochord of length ($L$) and linear mass ($\mu$), loaded by mass ($m$) attached at distance ($x$) to one end. The added mass reduces the root note ($f_0$) when we pluck or bow the string. Using these parameters, we can find the frequency shift for a given string:

$$x_r = x/L, \, m_r = m/(\mu * L), \, f_r = -df/f_0$$

When $x_r$ and $m_r$ are lower than 0.3, we can approximate the results using the following equation:

$$f_r(\%) = k * x_r * m_r, \text{ with } k = 500$$

Viola strings have a $\mu$ range from a maximum of 8 g/m for C to 1.4 g/m for A. The plastic



*Figure 2. Stiffness scaling and string holder.*

## Laser Position Sensor
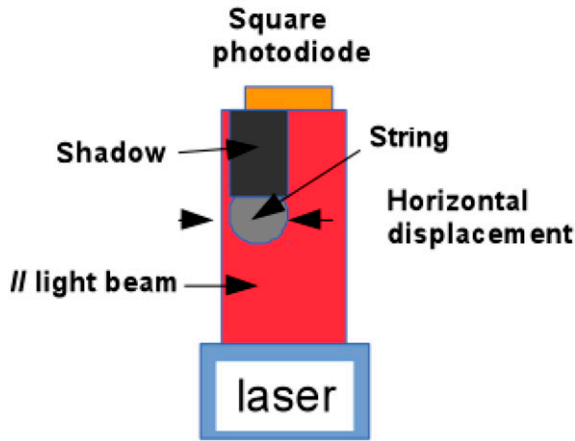


*Figure 3. LPS principle. A 5-mm diameter parallel laser beam impinges normally on a BSW34 PIN 2.35-mm square photodiode. The upper face, which is used for the bridge, intercepts approximately half of the beam that is aimed for the diode. For the strings, which are usually no more than 1 mm in diameter, we had to increase this diameter to ~3 mm by a set of 4-mm long black, thermally retractable tubes. When the string has a synthetic core, the user must use a flat iron tip at low temperature. The tube can slide, with some effort, along the string, after tuning, to reach the right position in front of the diode. The full-view photocurrent is measured on a 1-k$\Omega$ resistor. This voltage ($V_0$) normalizes the full scale. Each measured dV(t) corresponds to an elongation dx(t) = 2,650 * dV(t)/$V_0$ micrometers. The rms noise has a value of 0.5 µm. The frequency response is not a problem as it has a pin diode rise time less than 10 ns. A spinning shutter provides a V(t) response, which converts to V(x) using the precise tangential velocity. The mean slope is deduced with a 3% inaccuracy.*

*Table 1. Tube loading frequency reduction effect.*

| | L (cm) | $f_r$ % | |
| --- | --- | --- | --- |
| | | µ, max = 8 | µ, min = 1.4 |
| MS | $L_{max}$ = 37 | 0.2 | 1.3 |
| | $L_{min}$ = 15 | 1.4 | 7.9 |
| AS | $L_{max}$ = 20 | 0.8 | 4.5 |
| | $L_{min}$ = 7 | 6.4 | 36.4 |

in the C and G strings, which have a $\mu$ higher than 3 g/m. We verified this conclusion by repeating some records using balsa wood tubes, seven times lighter (3 mg). The three LPS simultaneously record the horizontal motion of the vibrating string and the AS at 20 mm from the holder, and the horizontal motion of the holder. A mechanical bow, with controlled velocity and pressure, excites the vibrating string within the normal range of playing. We built a special bow for this experiment by gluing a normal head and frog onto an 8-mm carbon fiber tube. A plastic wheel rolling over the tube is loaded vertically by adding lead pieces, which sets the pressure on the string, as seen in Fig. 4. As the bow moves, pressure varies, because of the bow mass contribution, from 1.1 N at the tip to 1.3 N at the middle. The bow translation is performed by using a low-noise direct current motor to turn a round-threaded screw on which is wound a carbon braided-wire loop, which in turn drives the frog. The motor axis position is monitored by a coupled potentiometer. Position and bow speed can also be precisely checked by a digital linear optical scale attached to the bow carbon tube. With a motor power supply range of 4–15 V, the up and down bow speed can be selected between 10 and 40 cm/s.

The rig plays the string by applying a roller as a player would apply a finger. A second DC-motor moves the roller along the fingerboard in fixed steps by turning a threaded rod attached to the roller, as seen in Fig. 1, thus reducing the vibrating length *L*. We use a 1.5-octave glissando, as used to analyze the effect of sound-post placement and bridge resonances [4]. The motor commands are synchronized in the following

tube weighs 25 mg for a length of 4 mm, and is placed at 2 cm from each side of the bridge. *L* varies, depending on measurements, from 20 to 37 cm on main string (MS) and from 7 to 13 cm on AS. Table 1 shows the frequency shift of $f_0$ induced by the tiny tube. This demonstrates the low impact that the tube has on the MS motion
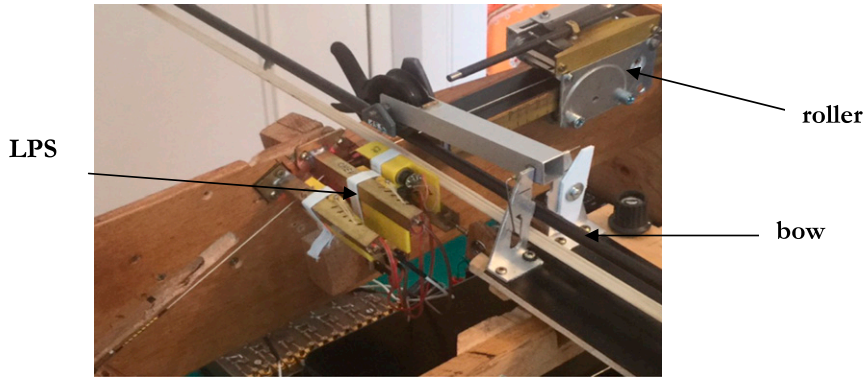
*Figure 4. LPSs setting, bow motion, and roller.*

typical sequence: down-stroke and roller for 1 s, stop 1 s, up-stroke for 1 s, stop 1 s, etc. The roller motor voltage is chosen to produce less than a semitone frequency variation per down-stroke, to achieve high frequency resolution when a 1.5-octave sweep is performed. A much lower voltage is used to delve around a resonance.

We adjust the LPS in front of the tubes at $V_{0/2}$ at rest, using the same response sign, to obtain the correct phase shifts between signals. We used computer-assisted analysis offered by the shareware Sigview to extract pertinent quantities, including amplitude, harmonic content, and phase shifts. As the motion signals $dV(t)$ are not sinusoidal, we calculated amplitudes in micrometers rms units.

$dV(t)$ rms = moving average of $(dV * dV)^{1/2}$ on 1,000 samples at a sample rate = 16 kHz ($dt$ = 62 ms) and $dx(t)$ micrometers rms = 2,650 ∗ $dV(t)$ rms/$V_0$, 2,650 being the linear range of the LPS in micrometers.

Unless we specify otherwise, the bowing has the following parameters: bow-hair ribbon 1 cm wide, with pressure of 1.2 N, and velocity of 19 cm/s.
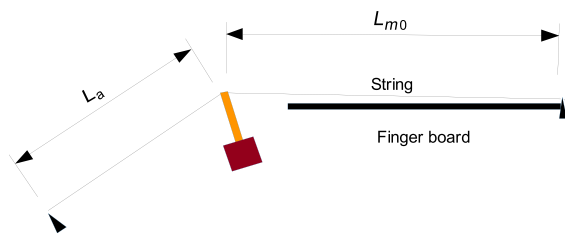


*Figure 5. Geometry.*

Data show the system consistently achieving ±1 dB results in both fidelity and stability over several months in use.

## RESULTS

### For One Bare String (Saddle to Nut)

While operating on the C string in blocked mode at 130 Hz, the holder cannot move (Fig. 5). The attached quartz force sensor (HFS) provides the force transmitted to the holder by MS (Fig. 6). The data clearly demonstrate the Helmoltz shape, similar to MS and the pressures which piezzo sensors demonstrate when placed under the feet of the bridge on a viola.

These data quantitatively verify the formulation of L. Cremer ([5], §3.4, equation number 3.22). We can calculate the peak force at the bridge using the equation:

$$F(0) = (Fx * m')^{1/2} * vb * L/xb,$$

where $Fx$ = tension, $m'$ = string linear mass, $vb$ = bowing speed, $L$ = string length, and $xb$ = bow–bridge distance. Here, $Fx$ = 58 N, $m'$ = 5.7 g/m, $xb$ = 2 cm, $L$ = 37.5 cm, and $vb$ = 19 cm/s. This provides a force $F(0)$ of 2.05 N.

The HFS measured $F(0)$ = (1.4 N/mV) ∗ 3 mV = 4.2 N, if we take the peak-to-peak measured values.

The holder also functions as a force sensor through its compliance. A sawtooth signal provides a peak to rms value of $3^{1/2}$ = 1.73. Here, BR/MS = 0.25 and MS peak to peak = 0.9 mm (see Table 2). As a result, $F(0)$ = $K$ * 0.9 * 0.25 = 4.3 N, as $K$ = 19.4 N/mm.
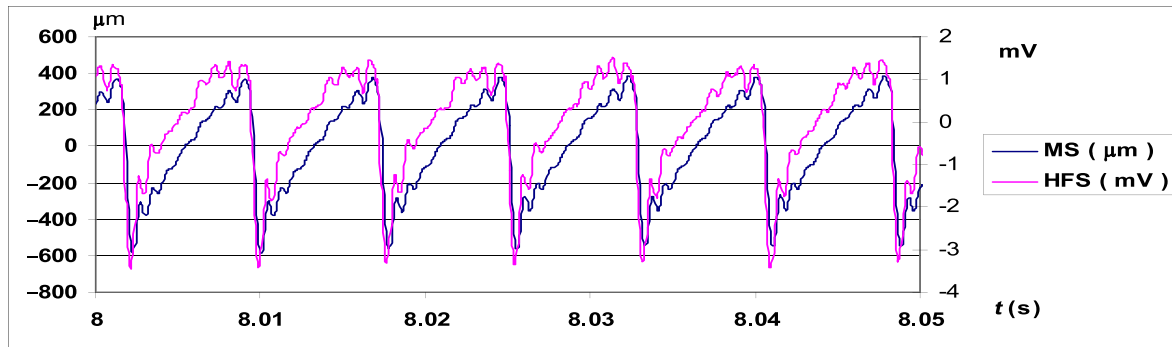
*Figure 6. Blocked mode: MS motion at 2 cm from holder and force on holder.*

The tests provide a generic record or the movements of a C string at pitch under arco (bowed) conditions (Fig. 7). These $dV(t)$ data demonstrate the motions of a MS of length ($L_m$), an AS of length ($L_a$), and simili-bridge (BR), recorded in 196 s and corresponding to a frequency span of 134–324 Hz. We tested an extra-long C string of 575 mm ($L_m$ = 375 mm and $L_a$ = 200 mm).

The analysis demonstrates that:

1. MS amplitude decreases slowly as the sweep increases from 134 to 324 Hz when the pull is 10% higher than the push (hair-scale effect),
2. AS resonances are strong with an amplitude that is often higher than that of the MS, with $L_m = L_a$ = 200 mm, and $L_m = 3/2 * L_a$, with Q ~ 100.

3. BR amplitude dips after the main AS resonance ($fr$ = 216 Hz). The data show a 5-dB loss in mean rms level on a semitone.

Displacements, which we have expressed in micrometers (rms), are shown in (Fig. 8).

The MS motion has many harmonics. Resonances occur based on the formula:

$$n * f = m * fr \,(1)$$

where $f$ is the played note and $fr$ is the first AS resonance frequency. At $f$ = 148 Hz, $n$ = 3, and $m$ = 2, AS vibrates at 432 Hz. At $f$ = 216 Hz, $n$ = 1, and $m$ = 1, syntonization occurs.

A very slow sweep near 216 Hz provides a closer look at the coupling process.

**Table 2. The first three columns demonstrate open string excitation. The fourth and fifth columns refer to the main 1–1 resonance. Note that a more flexible holder increases both amplitude and loss. This experiment used the following extra-long strings: Corelli-Alliance for the C and G strings, Helicore for the D string, and Jargar for the A string. Arco parameters were 19 cm/s at 1.2 N.**

| K holder (pseudo-bridge) | String | Amplitude MS open | AS/MS open | BR/MS open | AS/MS at reson | BR dip = dB − $df/f$ (cents) |
|---|---|---|---|---|---|---|
| | C | 260 | 0.35 | 0.25 | 2.6 | 5 – 65c |
| 19.4 N/mm | G | 176 | 0.4 | 0.23 | 1.6 | 4.2 – 75c |
| | D | 123 | 0.55 | 0.36 | 2.15 | 7 – 65c |
| | A | 77 | 0.5 | 0.45 | 1.6 | 3.5 – 65c |
| | | Microns | | | | |
| *K* holder-10.4 N/mm | C | 331 | 0.38 | 0.26 | 1.2 | 11 – 37c |

AS = after-strings; BR = pseudo-bridge; MS = main string.
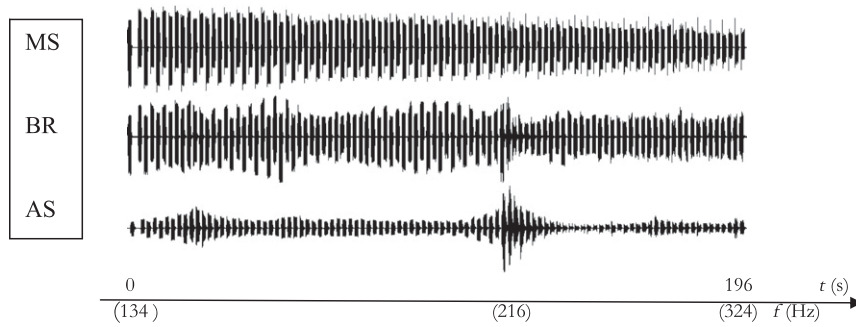
*Figure 7. Up to down MS, BR, AS recorded dV(t) signals given by LPS as a function of the roller travelling time. Notice that the frequency, 1/L dependent, does not increase linearly with time.*
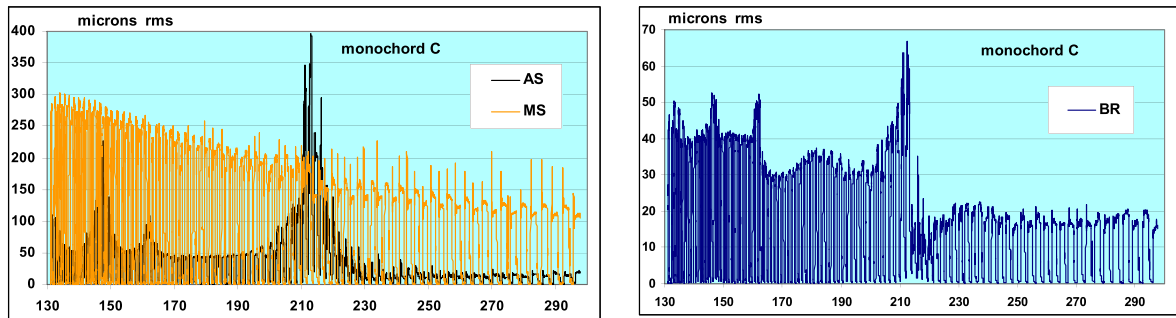


*Figure 8. Motion profiles as a function of MS frequency. The notes spacing increases as the string length reduces.*
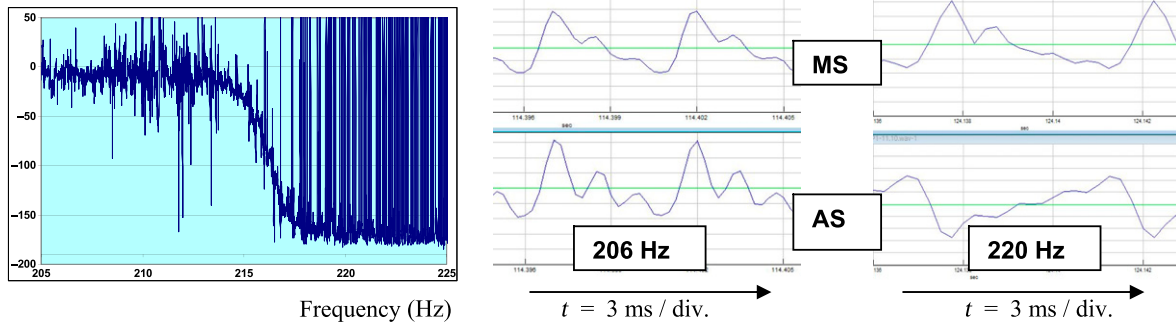


*Figure 9. Slow sweep. Phase shift between AS and MS fundamentals, from 205 to 225 Hz. The time signals show the "curve veering," after passing the resonance frequency at 216 Hz.*

Performing this sweep demonstrates the well-known phase shift between AS and MS harmonics near resonance and real time signals (Fig. 9):

1.  The phase shift on fundamentals is 0 at $f < fr$ and –180 degrees at $f > fr$. The bridge seems to act as a pivot, as if the string was stiff and transfers a significant part of the vibrating energy to the AS.

2.  The fundamental component of resonance is strongly present in BR.

Real time signals around $fr$ = 216 Hz demonstrate the phase shift reversal. While
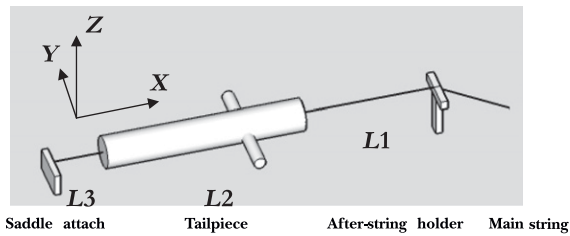
*Figure 10. Geometry.*

approaching *fr*, the AS helps the MS transfer energy to the bridge. Above *fr*, the effect slows down and deadens the bridge motion. This would cause a viola to emit a less intense A note. Similar situations occur for other strings, as summarized in Table 2.

### For Single Strings with Cylindrical Aluminum Tailpieces

We shortened the AS and loaded it with a pseudo-tailpiece (Fig. 10).

Lateral posts affix horizontally or vertically along the cylinder to increase mass and inertia. These can cover all shapes and materials used in conventional tailpieces. We measure inertia along the three axes using a torsion pendulum. To choose the correct mechanical parameters, we have measured commercial tailpieces and compared them with our set of three cylindrical aluminum samples. All devices had an *L2* = 100 mm. After-lengths (*L1*) of 7, 8, and 9 cm have been tested, with corresponding attachment cords with length (*L3*) of 3, 2, and 1 cm (Table 3).

To give an example of the data recorded, we present in Fig. 11 the three motions in arco condition on a C string, in micrometers rms, and in Fig. 12 the frequency shift vs. *L3*.

The bridge motion demonstrates the steps in the resonance when we excite the AS on partials *n* = 4, 3, and 2 of the MS. BR amplitude increases as we approach these frequencies and decreases afterward. This demonstrates the coupling effect explained previously.

### Tailpiece resonance

Bruce Stough [1] identified five tailpiece resonance modes on violins. The three lowest do not alter the response of the instrument, but the two highest make a strong difference. Chladni

*Table 3. Mechanical parameters for commercial and pseudo-tailpieces.*

| Viola type | Mass (g) | Length (mm) | Max width (mm) | Min width (mm) | Inertia (kg $*$ m$^2$) | | |
|---|---|---|---|---|---|---|---|
| | | | | | Jy | Jx | Jz |
| Standard ebony— 1 adjuster | 21.1 | 125 | 44 | 18 | $3.7 \times 10^{-5}$ | $3.0 \times 10^{-6}$ | $4.1 \times 10^{-5}$ |
| Ill rosewood—4 adjusters | 23.5 | 128 | 46 | 16 | $2.4 \times 10^{-5}$ | $1.7 \times 10^{-6}$ | $2.5 \times 10^{-5}$ |
| Wittner 916131 | 32 | 125 | 47 | 17 | $3.8 \times 10^{-5}$ | $3.5 \times 10^{-6}$ | $4.2 \times 10^{-5}$ |
| Cordiera assym pear tree— 3 adjusters | 10.7 | 130 | 30 | 16 | $1.6 \times 10^{-5}$ | $1.9 \times 10^{-6}$ | $1.7 \times 10^{-5}$ |
| Cordiera assym ebony— 3 adjusters | 13.5 | 130 | 30 | 18 | $1.3 \times 10^{-5}$ | $1.1 \times 10^{-6}$ | $1.4 \times 10^{-5}$ |

| Aluminum sample | Mass (g) | Length (mm) | Diam. (mm) | Jx | Jy,z |
|---|---|---|---|---|---|
| Al-1 | 7.2 | 100 | 6 | $3.3 \times 10^{-8}$ | $6 \times 10^{-6}$ |
| Al-2 | 11.7 | 100 | 8 | $9.2 \times 10^{-8}$ | $9.8 \times 10^{-6}$ |
| Al-3 | 26.5 | 100 | 11.3 | $4.2 \times 10^{-7}$ | $2.3 \times 10^{-5}$ |
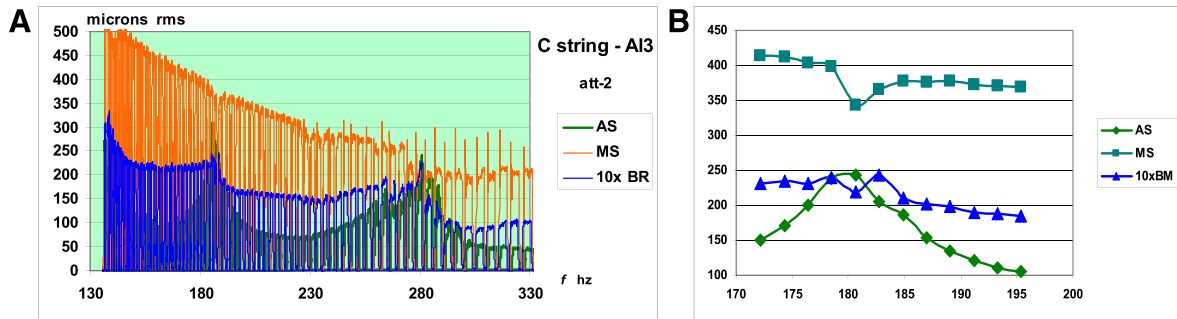
*Figure 11. A) Motion diagrams for after string AS, master string (MS), and bridge (BR) with the Al-3 tailpiece. B) Close-up view of the AS resonance at 550 Hz on partial 3 of MS (180 Hz).*
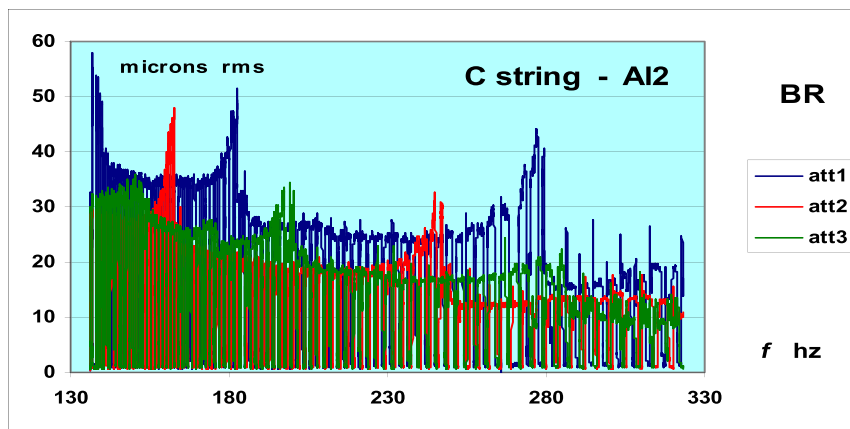


*Figure 12. Bridge motion as a function of att. of 1, 2, and 3 cm, with the Al-2 tailpiece.*

visualization was used under direct magnetic tailpiece excitation. Our experiment was performed with only one or two strings at pitch. When we pluck the AS near the tailpiece, the damped AS motion shows a very low resonance frequency (*fr′*) of the mass–string system. In all cases, *fr′* is lower than the open MS frequency, lower than 100 Hz for the C string. We have measured *fr′* for the bare aluminum cylinders and for the Al-2 tailpiece loaded with heavy H-shaped masses (Fig. 13).

+Pb: $m$ = 40 g, Jy = 7.8 e-5 kg $*$ m$^2$

+Brass: $m$ = 62 g, Jy = 10.5 e-5 kg $*$ m$^2$

If we load the aluminum cylinder with two brass posts of 30 mm, horizontally, adding 10 g

across the front of the cylinder, we observe a reduction of *fr′* for any MS string (Fig. 14).

Under the same pluck, the horizontal tail motion is recorded by an LPS placed at various positions along the cylinder: "front" means bridge side and "back" means saddle side. The tailpiece resonance frequency is close to *fr′* (Fig. 15). In addition, we observed that the tail motion is always out of phase with the holder.

*After-length string resonance*

Next, we examine AS resonance under MS arco conditions (Fig. 16).

Interestingly, this *fr* seems to be independent of the mass or inertia of the tailpiece within the range of tested parameters. We find that *fr* is between 10% and 20% lower than $fr_0$, calculated for an AS fixed at both ends:
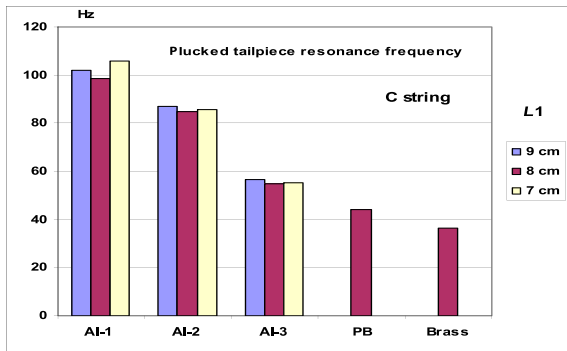
*Figure 13. Resonance frequency fr′ obtained from plucking the AS. Pb and Brass loading of Al-2.*
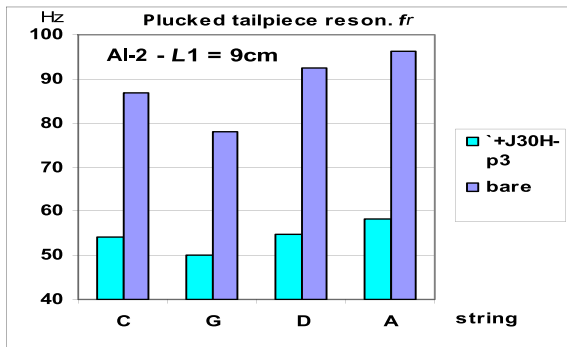


*Figure 14. The impact of adding lateral posts to the Al cylinder on the resonance frequency.*

$$fr_0 = 1/(2 * L1) * (Fx/mu')^{1/2},$$

where according to *L*. Cremer notations [5], *Fx* = tension and *mu′* = linear mass.

The *fr* reduction comes in part from the tube loading effect and in part from the silk end. This reduction is observed for the large inertia range investigated (Fig. 17).

As the AS mass is always less than 5% of the tailpiece mass, we infer that the tail provides an almost fixed point, even when including four string tension.

### The effect of the attachment cord

Violinmakers often espouse that a more flexible attachment would improve the sound by leaving more freedom for the bridge to move. We have tested this notion by comparing three cases. The first configuration has one thin carbon braid with $\phi$ = 0.2 mm. The second has two parallel thicker braids with $\phi$ = 1 mm. The third has a fixed metal strip which connects the body on one end to the cylinder via a vertical pivot point. We tested three cord lengths with attachment lengths (att.) = 1, 2, and 3 cm and corresponding AS lengths of 9, 8, and 7 cm. We plotted, in Fig. 18, the results for four among the nine cases, for an 11.7-g Al-2 tailpiece (fine and metal cords, att. 1 and 3 cm). The frequency sweep shows almost equal amplitudes and similar modulation in the bridge motion, with larger resonances on shorter cords. A heavier 27.5 g Al-3 tailpiece smooths the BR undulations.

In conclusion, the cord att. is a way to adjust the AS resonance frequency, but has no effect on the bridge motion.
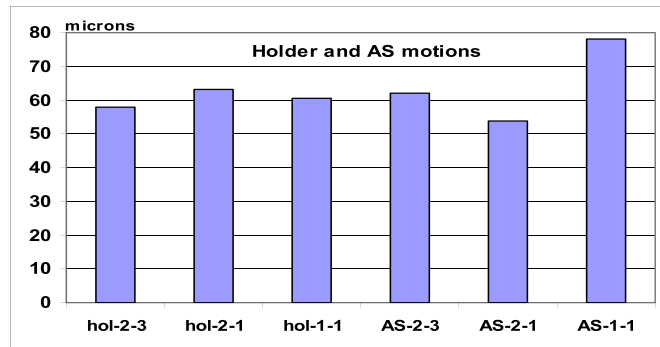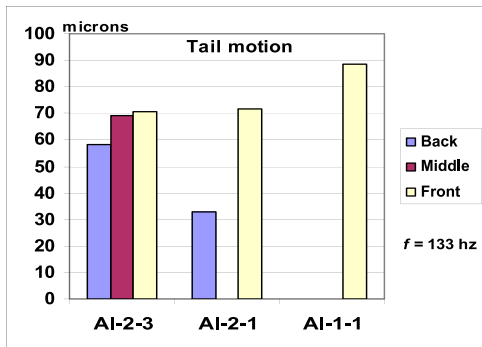


*Figure 15. Left graph shows the horizontal tail motions, in micrometers rms. Right graph shows the corresponding holder (hol) and AS motions. Conditions: open C string (133 Hz) and an unloaded tailpiece. Coding: first indice = tail type, second indice = cord length, L3.*
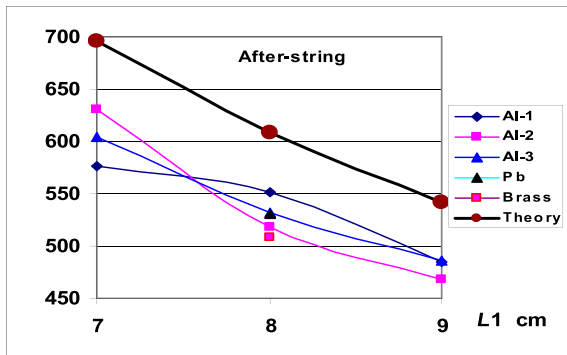
*Figure 16. AS resonance frequencies fr.*

### Harmonic enhancement

In all cases, spectral analysis of the BR motion reveals local enhancement of its partials when they coincide with the AS resonance frequency (*fr*).

## For Two Strings Attached Symmetrically or Asymmetrically to a Cylindrical Aluminum Tailpiece

Next, we attach a second string to the side of the pseudo-tailpiece. Here, the lower notes have longer after-lengths (Fig 19). The multiple strings on the bridge increases the number of coupled resonators. We now measure five motions.

Carleen Hutchins was the first to suggest the adjustment of the sympathetic vibrations of the ASs to the harmonics of the open strings as a way to modify the sound [6]. For some years, "Cordiera Cantabile" has promoted triangular shaped tailpieces. These tailpieces adjust the after-length of strings at a fixed ratio between the notes played in the back and front of the bridge (Fig. 20). We call this ratio
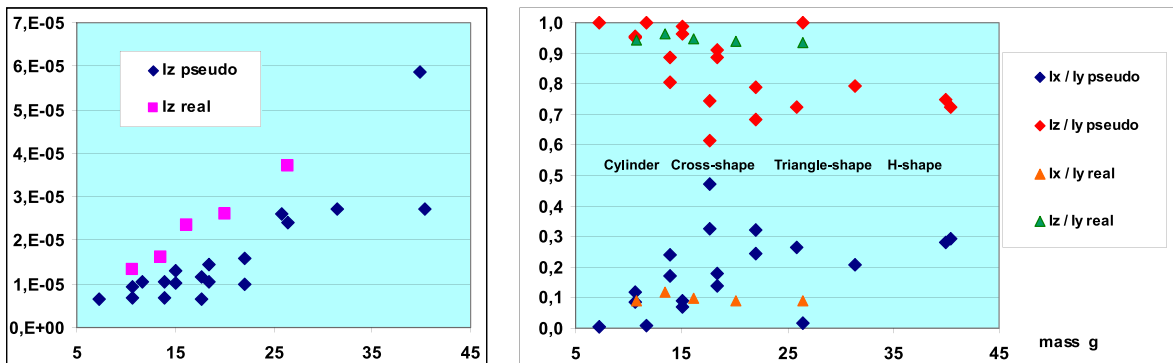


*Figure 17. Inertia range investigated, as a function of tailpiece mass. "Real" refers to the commercial tailpieces shown in Table 2.*
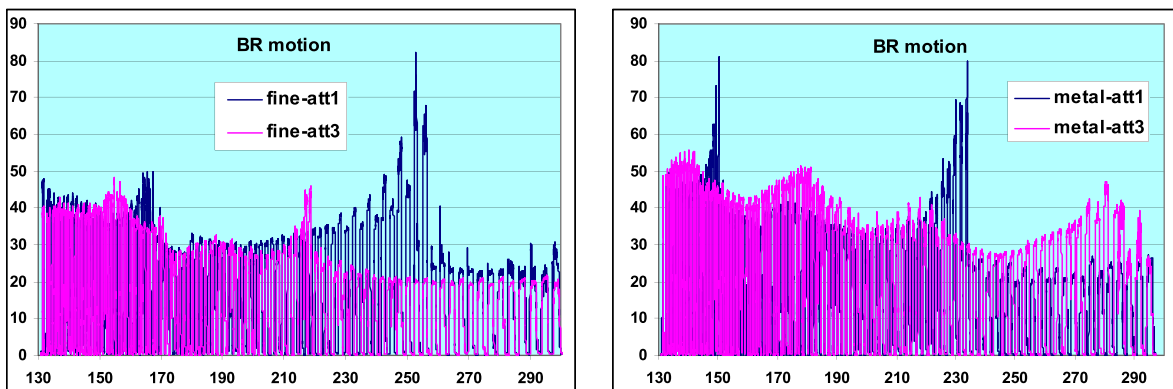


*Figure 18. BR motion sensitivity to attachment cord type. Al-2 tailpiece—C string—sweep from 135 to 305 Hz. Fine set at one thin braid, att. = 1 for cord length = 1 cm.*
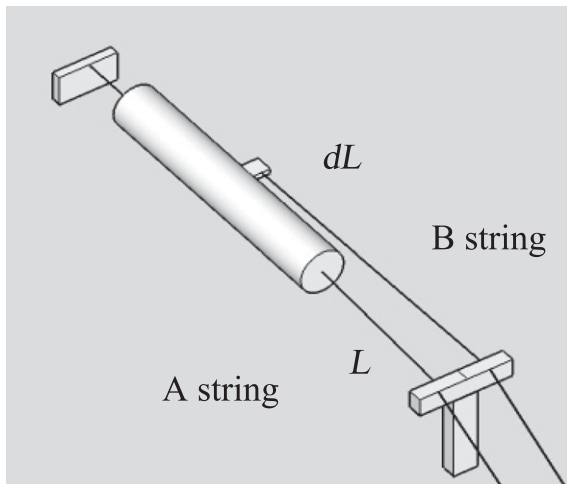
*Figure 19. String B is longer than string A: dL.*



*Figure 20. Viola cordiera cantabile tailpiece.*

the "mode." The mode can, for example, be 3, 4, 5, and 6 for strings IV to I. This design intends to free the bridge from the suspected damping effect of short AS lengths. Acoustical measurements and auditions, performed on violins, violas, and cellos, have shown this tailpiece to produce a warmer tone and better expressiveness, particularly for the III and IV strings.

Our goal here is to investigate the influence of $L1$, $dL$, and the att. on holder motion. For clarity purposes, we are only reporting results obtained on a C string with $L + dL$ = 140 mm, coupled to a G string with $L$ = 95 mm and att. = 10 mm. We used the Al-2 tailpiece to set mass and inertia. We played the C string, and

then the G string, and recorded all motions (Fig. 21).

Modulations in the holder motion amplitude (BR) occurs in steps, as seen before in a single string configuration. We localized transition zones at ±1 tone. The MSs resonate at their fundamental or harmonic frequencies when other strings are sounding at harmonic combinations. Soloists experience this frequently. As before, the $fr_0$ data shown in Fig. 21 is within 85–94% of the theoretical values. Doubling the string's tension slightly increases the lowest resonances of the tailpiece ($fr'$) to more than 108 Hz. We can then infer that when four strings are attached and even when using light tailpieces, normal play will not excite this lowest mode. We obtain similar results with the G–D pair. If we play the C string, coupled successively to the G, D, and A strings, we reveal the impact on the BR and the open strings (Fig. 22).

Mean BR motion holds near 30 µm, but added steps shift in frequency. Only the AS-C resonance impacts the BR motion when coupled with the G string. The D and A open strings only create resonances leading to bridge steps.

We now consider an instrument from the violin family, fitted with four strings and tuned in fifths with an asymmetric tailpiece adjusted to the 3, 4, 5, and 6 modes. Vibrational energy flows from the bowed string to the body and the present resonators (Fig. 23).

The simulation is carried out by playing the 13 rising chromatic notes, numbered 1 to 13, of one octave on each I–IV string, and all the possible resonances up to the 10th partials are recorded. Table 4. The lowest note is normalized to 1.

As the partial levels decrease in 1/$n$, we extract the h1 or h1 + h2 as modulating candidates. These sums indicate three or seven modulations in ASs and five to eight modulations in open strings. If we compare this with a standard tailpiece with a mode of six for all strings, only the AS-IV coupling of 11 h1's exists, which is a G# bowed on an A string. These amplitudinal and tonal modulations are transmitted via the bridge to the body, matching to the air through impedance transfer function. The body itself, as a complex resonator, does not interfere with bridge motion unless a very strong coupling occurs [5].

## C string bowed          ## G string bowed
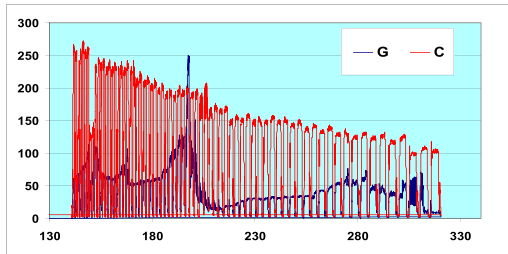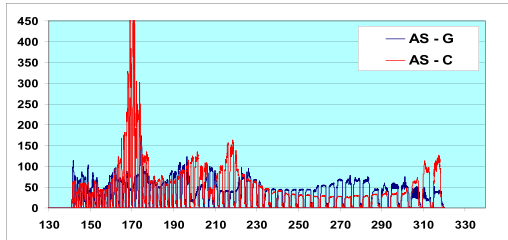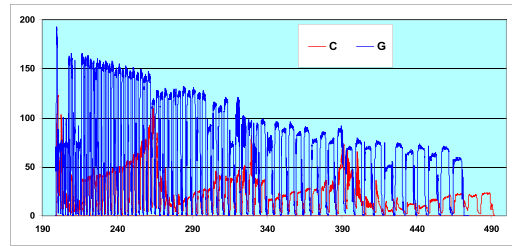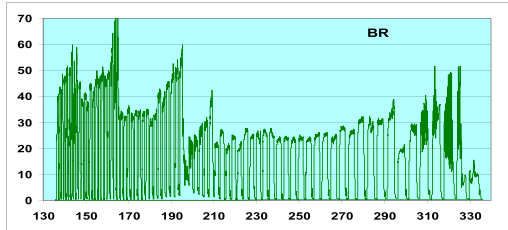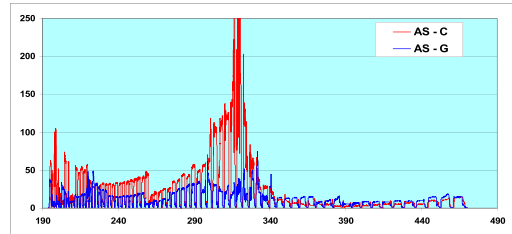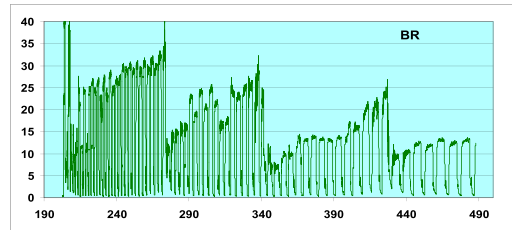


| MS | AS | BR |

| | Resonances | | | Step BR |
|---|---|---|---|---|
| *f* - C string | G | AS - C | AS - G | |
| bowed | *fr*$_0$ = 193 | *fr*$_0$ = 322 | *fr*$_0$ = 662 | |
| 145 | 4-3 | | | |
| 165 | | 2-1 | | |
| 195 | 1-1 | | | |
| 209 | | 3-2 | | |
| 326 | | 1-1 | | |

| | Resonances | | | Step BR |
|---|---|---|---|---|
| *f* - G string | C | AS - C | AS - G | |
| bowed | *fr*$_0$ = 130 | *fr*$_0$ = 322 | *fr*$_0$ = 662 | |
| 194 | 2-3 | 3-1,8 | 3-1,1 | |
| 207 | | | | |
| 227 | | 3-1 | 3-1 | |
| 255 | | 4-3 | | |
| 274 | 1-2 | | | |
| 306 | 2-1,1 | | 2-1,1 | |
| 314 | 3-7 | | | |
| 322 | | 1-1 | | |
| 333 | 2-5 | 2-1 | 2-1 | |
| 341 | | | | |
| 372 | 2-6 | | | |
| 427 | min level | | | ? |

*Figure 21. Resonance summary for the C and G string assembly. L$_1$ = 95 mm. L$_1$ + dL = 140 mm. Att. = 10 mm. fr$_0$ indicates the resonance frequencies of the open string and after-length strings. The tables list the peak motion frequencies observed on each resonator, expressed by the n–m partial factors involved in Eqn. (1) at the corresponding bowed string frequencies f. Green steps show where we observe bridge motion reduction. Note that the frequencies of the bridge steps coincide with the G or C AS when we bow C. Step positions are just above the resonances which occur when we bow G. In the last case, we observe combined resonance.*

**Played note on C string, in Hz**



**C – D string pair**



**C – A string pair**

| f - C string | Resonances | | | | | | |
|---|---|---|---|---|---|---|---|
| | AS-C | G | BR - G | D | BR - D | A | BR - A |
| | $fr_0 = 322$ | $fr_0 = 193$ | | $fr_0 = 293$ | | $fr_0 = 440$ | |
| 145 | | 4-3 | | 2-1 | | 3-1 | |
| 161 | 2-1 | 2-1,66 | | | | | |
| 166 | | | | | | | |
| 171 | | | | | | 5-2 | |
| 179 | | | | 3-2 | | | |
| 191 | 3-1,75 | 1-1 | | | | | |
| 203 | | | | | | | |
| 210 | | | | | | | |
| 217 | | | | | | 2-1 | |
| 277 | 2-3 | 2-3 | | | | | |
| 283 | | | | 1-1 | | | |
| 323 | 1-1 | | | | | | |

BR step origin   BR step position

$fr_0$ AS - D = 1031   $fr_0$ AS - A = 1133
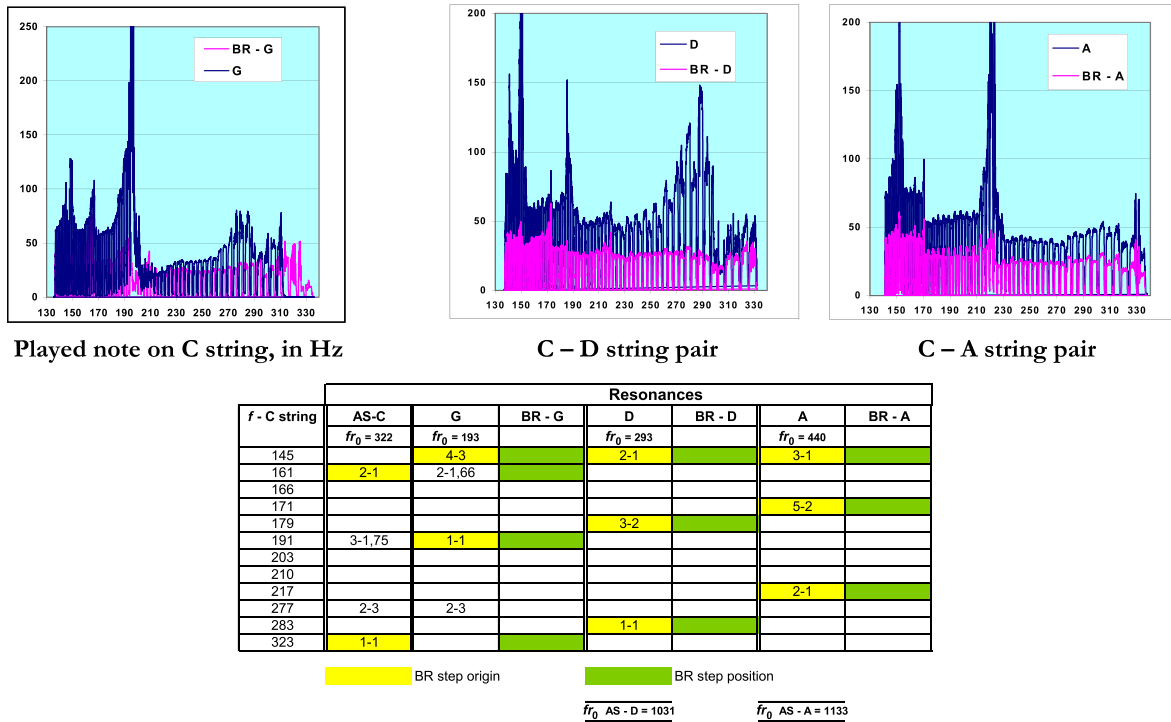
*Figure 22. Peak resonances which occur when coupling the bowed C string with other open strings. Each cell uses n ∗ (f) = m ∗ (fr₀).*

During the sixteenth century, viola makers fitted violas d'amore with eight sympathetic strings, which they tuned to add a reverberant and rich sound to the instrument. The Indian sitar and sarangi similarly use sympathetic strings to achieve a rich sound.
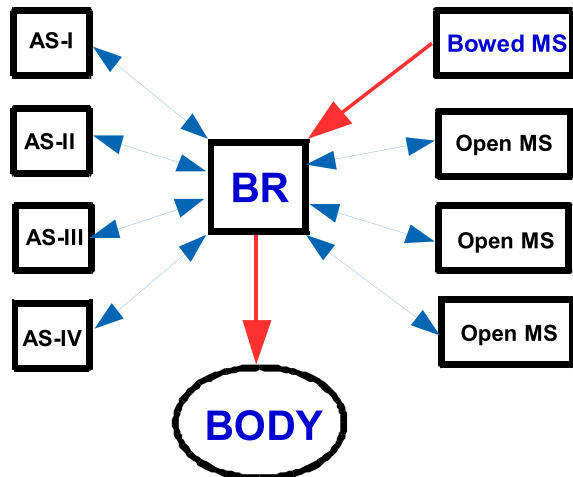


*Figure 23. Energy flow from bowed string to the body, including all present resonators.*

## DISCUSSION

What can we conclude from our measurements of the tailpiece's effects on the transmission of energy to the body? First, the physical design parameters of the tailpiece, such as mass and material, are not relevant at first to bridge motion. Rather, adjusting mass or position can shift the frequency of all resonant modes of the back bridge system, as identified previously by White et al [3]. Second, previous works have looked for tailpiece resonances by direct excitation by hammer tapping [2] or using magnets [1], and have discarded the correlation with the bridge's induced motion. I suspect that these methods can lead to the identification of modes that do not appear strongly when excitation comes from the horizontal bridge motion. However, the parameter sensitivity analysis of tailgut or AS lengths, performed by Stough [1], is confirmed

*Table 4. Normalized resonances between the bowed spectrum and open or after-length strings. Each cell provides the first played note and its corresponding partial. For example, 8-h2 on a viola's C gives a G (196 Hz), whose the second partial excites the AS-IV mode (3 × 131 = 393 Hz).*

| MS bowed | IV | III | II | I | h1 | h1 + 2 |
|---|---|---|---|---|---|---|
| After string resonances | | | | | | |
| AS-mode | 3 | 4 | 5 | 6 | | |
| AS-IV | 8-h2 | 13-h1 | 6-h1 | 11-h1 | 3 | 4 |
| AS-III | 8-h4; 4-h5 | 13-h2; 6-h3 | 6-h2 | | 0 | 2 |
| AS-II | 7-h8; 5-h9 | 12-h4; 8-h5; 5-h6; 2-h7 | 10-h3; 5-h4 | 10-h2; 3-h3 | 0 | 1 |
| AS-I | | 10-h8; 8-h9; 6-h10 | 8-h6; 5-h7; 3-h8 | 8-h4; 4-h5 | 0 | 0 |
| | | | | Sum | 3 | 7 |
| Open main string resonances | | | | | | |
| MS coupled | | | | | | |
| IV | | 6-h1 (h1/2) | | | | |
| III | 8-h1 | | 6-h1 (h1/2) | | 2 | 2 |
| II | 3-h2 | 8-h1 | | 6-h1 (h1/2) | 2 | 3 |
| I | 3-h3 | 3-h2 | 8-h1 | | 1 | 3 |
| | | | | Sum | 5 | 8 |

AS = after-strings; MS = main string.

here and quantified. Third, we find that the large number of amplitude and tone modulations present in the bridge have a localized frequency of 1 tone and a modest amplitude of 6 dB. A resonant body, however, can strengthen these modulations. Fourth, we have found that tailpiece asymmetry does not modify the mean sound intensity, but rather adds harmonic content in the lower range of frequencies. Could the withdrawal of the tailpiece system be a way to clear a lot of after-string length resonance problems? This idea would deserve to be discussed.

## ACKNOWLEDGMENT

| Glossary | |
|---|---|
| AS | After-string |
| MS | Main string |
| BR | Pseudo-bridge (holder) |
| $L_{m0}$ | MS open string length |
| $L_m$ | MS vibrating length |
| $L_a$—$L_1$ | AS length |
| L2 | Pseudo-tailpiece length |
| L3 | Attachment cord length |
| dL | Extra AS length |
| $f_0$ | Open string frequency |
| fr | AS resonance frequency |
| fr' | Low resonance frequency of the tail-AS system |
| mu' | Linear spring mass |
| LPS | Laser position sensor |
| HFS | Horizontal quartz force sensor |

## REFERENCES

[1] B. Stough, The lower violin tailpiece reso-nances, *CASJ*, Vol. 3, No. 1(Series II), pp. 17–25 (May 1996).

[2] E. Fouillhe, G. Goli, A. Houssay, and G. Stoppani, The Cello Tailpiece: How it Affects the Sound and Response of the Instrument. Proceedings of the Second Vienna Talk, Sept. 19–21, 2010 (University of Music and Performing Arts, Vienna, Austria).

[3] T. White, Telling tails, *The Strad*, Accessories Supplement 2012, pp. 8–13 (Oct. 2012).

[4] O. Rodgers, Effect of sound post adjust-ment, *CASJ*, Vol. 3, No. 3(Series II), pp. 19–23 (May 1997).

[5] L. Cremer, *The Physics of the Violin* English translation by The MIT Press, Cambridge, Mass. 1984. Original Edition under the title "Physik der Geige", S. Hirtel Verlag, Stuttgart, 1981.

[6] C.M. Hutchins, The effects of relating the tailpiece frequency to that of other violin modes, *CASJ*, Vol. 2, No. 3(Series II), pp. 5–8 (1993).